Design and Optimization of an Axially-Slitted High-Speed Solid Rotor Induction Motor

Ahmet Hakan OGUZ, Mehmet Onur GULBAHCE, and Derya Ahmet KOCABAS

Dept. of Electrical Engineering, Istanbul Technical University, Istanbul, Turkey
oguzah@itu.edu.tr, ogulbahce@itu.edu.tr, kocabasde@itu.edu.tr

Abstract

Axially-Slitted Solid Rotor Induction Motor (ASSRIM) has a better electric and electromagnetic performance in comparison to Smooth Solid Rotor Induction Motor (SSRIM) in high-speed drive application. A better flux penetration into rotor and increased rotor cooling capability can be performed with axial slits on rotor. The main drawbacks of the axially slits are decreased rotor bending resistance and increased air friction losses.
In this study, 20.5 kW, 23600 min^{-1} high-speed ASSRIM is designed and geometric design parameters of slits such as slit depth and width are optimized by finite element method (FEM). In order to determine optimal geometrical parameters, desired parameters are changed in order; others are kept constant while one is being optimized. 2D transient magnetic model is used for optimization.

Index Terms—*high speed induction machine, solid rotor, rotor slitting, slit optimization*

1. Introduction

In recent years, improvements industry technologies bring about an increase in optimal operation speed in drive systems. In this respect, recently developed high speed gearless or direct drive electrical drives are currently very trendy based on the reduction in the total structural volume of the drive system. Total structural volume is related to electromagnetic torque of electrical machine. Electromagnetic torque production is inversely proportional to the supply frequency. Due to the significant development of cost-effective, fast switching and compact variable frequency drives technology, wide speed range operations of different type AC motors has become feasible [1].

Solid rotor is mainly made of one type ferromagnetic material as single-piece. Due to their single material rotor structure and high thermal properties, Smooth Solid Rotor Induction Machines (SSRIM) are easy to manufacture, cost-effective and reliable alternatively to other types of high-speed machines [2]. In addition, even if they operate in high speed, they have low level of noise and vibrations. Another main advantage of this motor type is the ability to operate without a speed sensor unlike most of Permanent Magnet Machines [3].

Smooth solid rotor is the earliest and simplest rotor type for SRIM and it has the best mechanical and fluid dynamical properties. Due to result of skin effect and travelling eddy currents at the surface of ferromagnetic rotor material, it has the poorest electromagnetic characteristic. Since, magnetic flux penetration into rotor is low; the torque producing eddy-currents are concentrated on the surface layer. Furthermore, the rated slip value tends to be higher, rotor losses are high and power factor is low.

In literature, there are several methods in order to improve the performance of the (SRIM) [2, 4, 5]. One of the methods is placing copper end-rings on the end faces of the solid rotor body. The eddy currents tend to flow more aligned in the solid rotor body and the produced electromagnetic torque is doubled when compared with that of two pole smooth solid rotor without end-rings [2].

Most important contribution to improve performance of SRIM is axially-slitting on rotor body [2]. A better flux penetration and better eddy current distribution in the rotor can be provided by axially-slitting. This leads to increase the induced electromagnetic torque of electric motor and decrease the rotor losses caused by time and spatial harmonics [6]. Furthermore, slitting of the rotor increases the cooling capability of rotor. However, it increases the friction between air and rotor and it decreases the robustness of rotor [7]. Therefore, the optimization of the slit geometry parameters plays a significant role on decreasing rotor losses and increasing electromagnetic torque production.

In this study, firstly, a 20.5 kW, 23600 min^{-1} high-speed ASSRIM with copper end-rings is designed and analyzed by FEM. 2D transient magnetic model of ASSRIM is used for optimization process. Rotor correction factor calculations are also given. In order to obtain the best electromagnetic performance, geometrical parameters of slits such as slit depth and width are optimized by means of FEA. Designed motor is analyzed at thirteen different slit depths and ten different slit widths to determine the optimum slit structure by using 2D transient magnetic model and the results are presented in Section III and IV, respectively. Magnetic flux density distributions, magnetic flux lines distributions of rotor are represented for the obtained optimal rotor design after related optimizations.

2. 2D Transient Magnetic Model

In order to obtain optimal rotor parameters, previously designed [8] 15,5 kW 225V/400Hz 23600 min^{-1} SSRIM has been used as reference with its geometric quantities. All operational and geometrical quantities of based motor are given in Table. I. Rotors of both designs are made of steel-1010 and stator core is kept unchanged that is made of M350-50A. In this study, modelled rotor has an axially slitted cylindrical shape and the number of slits is chosen 28 in order to reduce the magnetic noise, since the slitted bars behaves like slots in a standard cage induction motor [9]. Unlike the traditional squirrel cage, rotor is heavily influenced by skin effect due to high operating frequency range. In order to obtain more accurate results, skin depth based mesh algorithm is used on rotor surface and teeth.

2D transient magnetic model and mesh structure of the initial slitted design are given in Fig. 1.

Table 1. Geometrical properties and rated values of SSRIM

Symbol	Quantity	Value
P	Rated Output Power	15.5 kW
V	Rated Voltage	225 V
I	Rated Current	65 A
F	Rated Frequency	400 Hz
2p	Number of Poles	2
n_r	Speed of rotor	23600 min^{-1}
S	Slip	1.7%
Q_s	Number of stator slot	24
Q_r	Number of rotor slit	28
D_i	Inner diameter of stator	0.1m
D_{out}	Outer diameter of stator	0.205m
D_2	Diameter of rotor	0.0985m
L_i	Total length of rotor	0.1m
k_{fe}	Stacking factor	0.96

ASSRIM have 98 wires per slot, 14 wires in parallel in which 0,8 mm diameter. Number of turns for each phase winding is equal to 7. The resistance of per phase winding is 26 mΩ and leakage inductance 68.4 µH at 400 Hz, 20 ^{o}C.

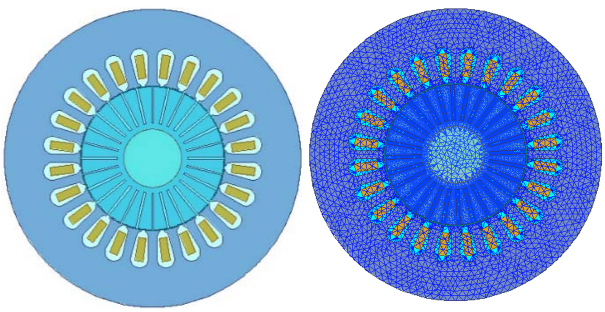

Fig. 1. 2D Transient Magnetic Model of ASSRIM and its skin depth mesh structure of the initial design

Because of decreased low frequency impedance of rotor depending on axial slitting [10], ASSRIM produces more torque at stable operation region at the expense of a decrease in pull-out torque. In addition to that, slitting the rotor increases high frequency surface impedance of the rotor. Therefore, rotor eddy current losses which are caused by time and spatial harmonic decrease [3].

The 3D rotor end-effects without using copper end rings are taken into account in the 2D transient magnetic computation by changing of rotor core resistivity in order to obtain more accurate results. This method is proposed by Russell [11]. The rotor core resistivity ρ_R is increased by a general equivalent end effect factor k_e to consider the existence of rotor end ring as given in equation (1).

$$\rho_R' = k_e.\rho_R \quad (1)$$

Without end rings $k_e=\alpha$ and with end rings k_e are used according to equation (2)

$$k_e = 1 + C.(\alpha - 1) \quad (2)$$

where C=0.3 for thick copper end rings which can be determined experimentally [2] and the coefficient α is represented equation (3)

$$\alpha = \frac{1}{k_R} = \frac{1}{1 - \frac{2.\tau_p}{\pi.l_{Fe}} \tanh\left(\frac{\pi.l_{Fe}}{2.\tau_p}\right)} \quad (3)$$

where k_R is Russell factor, τ_P is pole pitch, l_{Fe} is active rotor length [11].

3. Slit Depth Optimization

It is well-known that poor electromagnetic characteristics of (SSRIM) can be enhanced by axially-slitting the rotor [2]. The flux penetrates deeper on the slitted solid rotor in comparison to smooth solid rotor and the reluctance for tangential path increases. Since, the deeper flux penetration leads to induced current penetration resulting in an increase in induced electromagnetic torque at low slip values.

In this study, initial smooth rotor geometry divided by 28 slits having 1.5 mm width. In order to optimize slit depth, 12 different slit depths which are 2, 4, 7, 10, 13, 16, 19, 22, 25, 28, 31, 34 mm are analyzed at constant number of slits and 1.5 mm slit width by means of FEM. During the analysis slip kept constant at 1.7%.

It can be seen that Fig. 2, until an optimum slit depth, the electromagnetic torque increases with the increasing slit depth. As illustrated in Fig. 3, FEA results show that the optimal slit depth occurs at quarter of the diameter of the rotor since maximum electromagnetic torque with minimum supply current is seen at 25 mm slit depth.

Moreover, for a better visual comparison, magnetic field density distribution and magnetic flux lines distributions are given in Fig 4, 5, 6 for three different slit depths such as 0 mm, 13 mm and 25 mm.

4. Slit Width Optimization

Slit width is an important design parameter as slit depth. In order to find the optimum slit width for previously designed SSRIM, numerous simulations are performed by FEA for 10 different slit widths between 0.25 mm and 2.5 mm while keeping the previously optimized slit depth of 25 mm, the number of slits of 28 and slip of 1.7% constant.

As illustrated in Fig. 7 electromagnetic torque rises up to optimum slit width, than it decreases for wider slits. Since tangential component of leakage flux rises at thin slit, electromagnetic torque reduces. In addition, related to the reduction in rotor mass caused by larger slit width than the optimum one, distribution and density of eddy current is affected and electromagnetic torque also reduces.

As it can be seen in Fig 8, minimum input current with maximum electromagnetic torque occurs at 1.5 mm and it is chosen for optimal design. In order to obtain a visual comparison, magnetic field density distribution and magnetic flux lines distributions are given in Fig. 9, 10, 11 for three different slit width such as 0.25 mm, 1.5 mm and 2.5 mm.

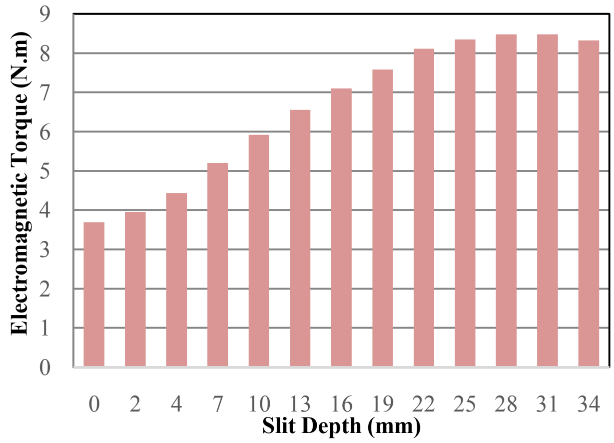

Fig. 2. Changing of electromagnetic torque with slit depth

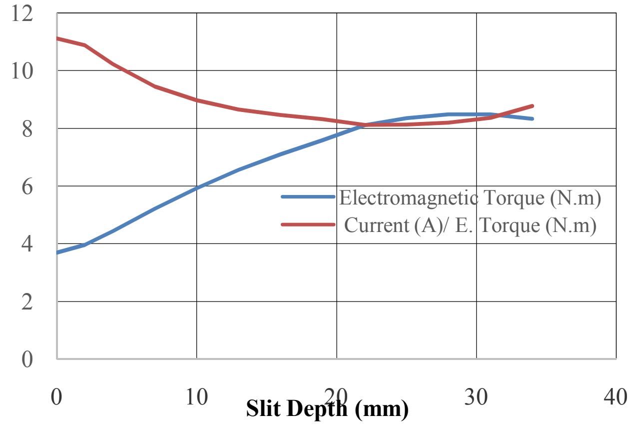

Fig. 3. Change of electromagnetic torque and stator current/electromagnetic torque versus slit depth

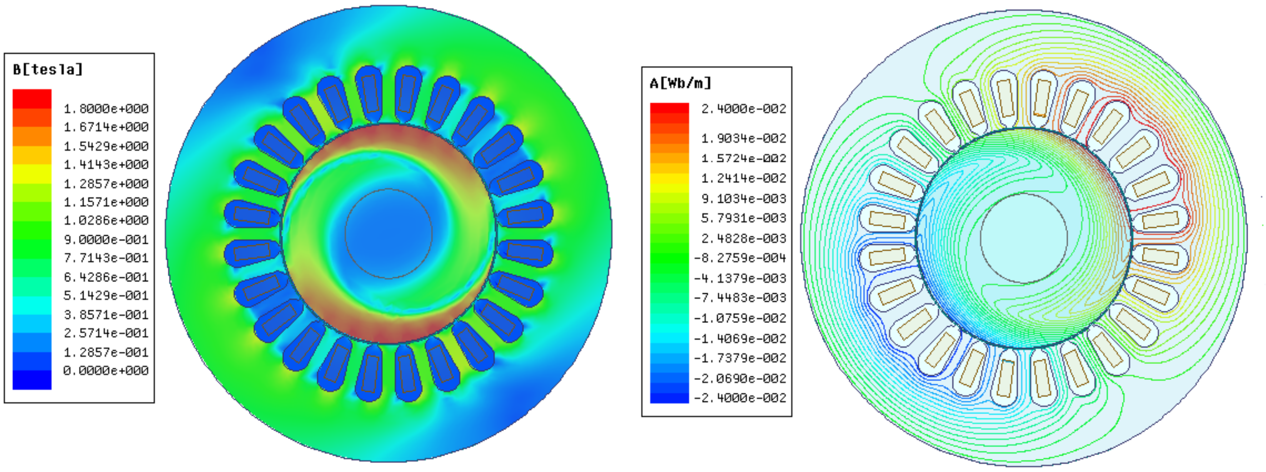

Fig. 4. Magnetic field density and magnetic flux lines distribution of SSRIM

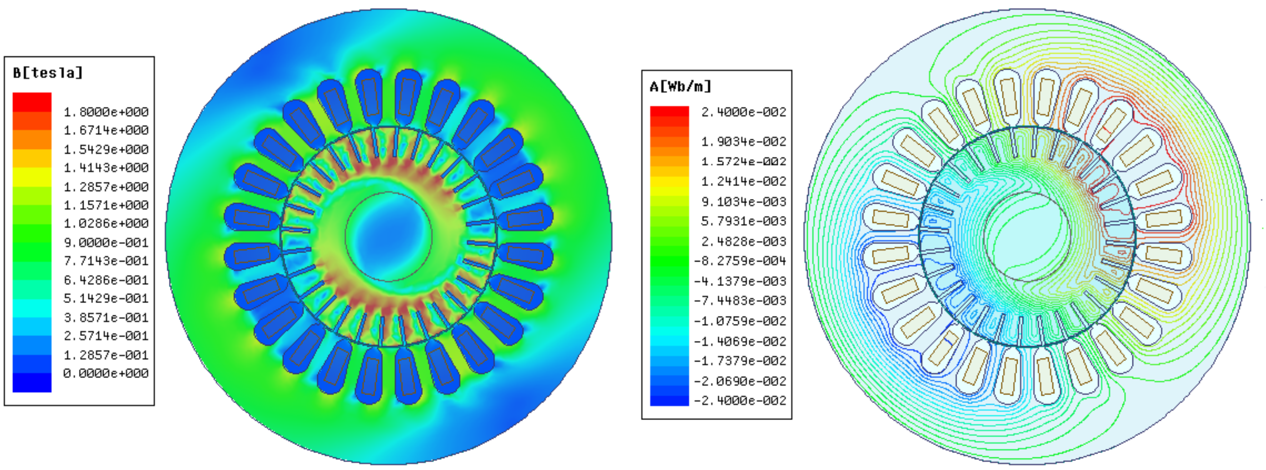

Fig. 5. Magnetic field density and magnetic flux lines distribution of ASSRIM with 13 mm slit depth

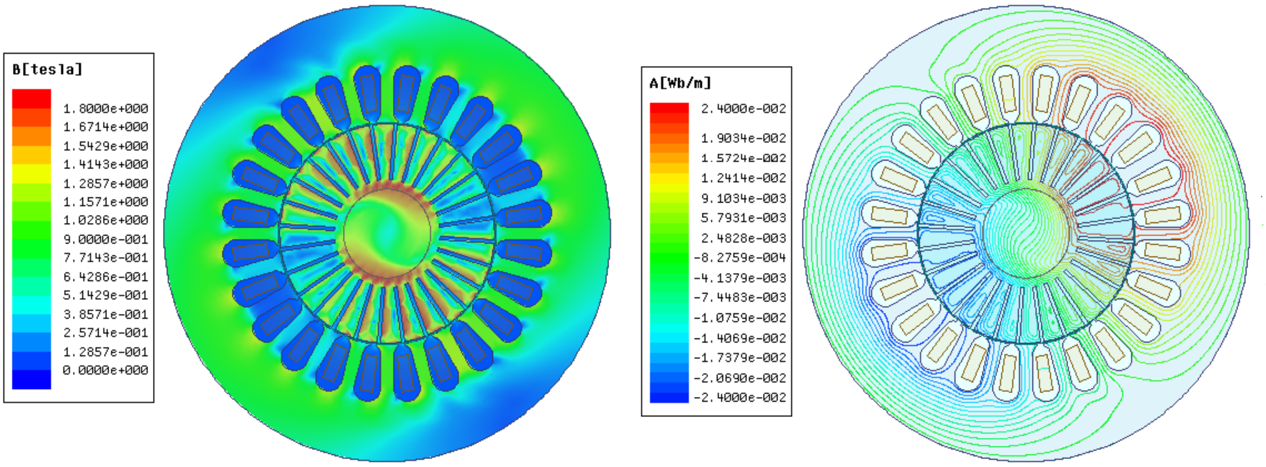

Fig. 6. Magnetic field density and magnetic flux lines distribution of ASSRIM with 25 mm slit depth

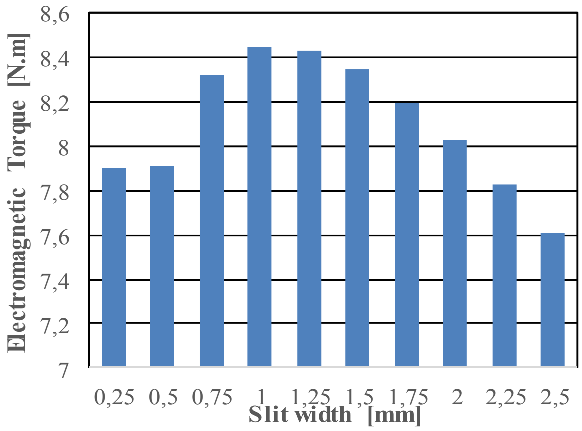

Fig. 7. Changing of electromagnetic torque with slit width

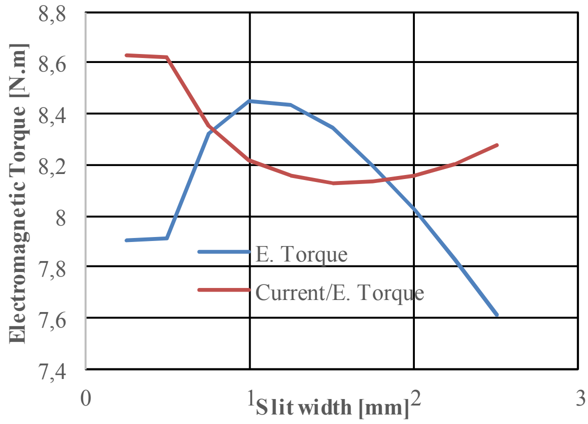

Fig. 8. Changing of electromagnetic torque and stator current/electromagnetic torque with slit width

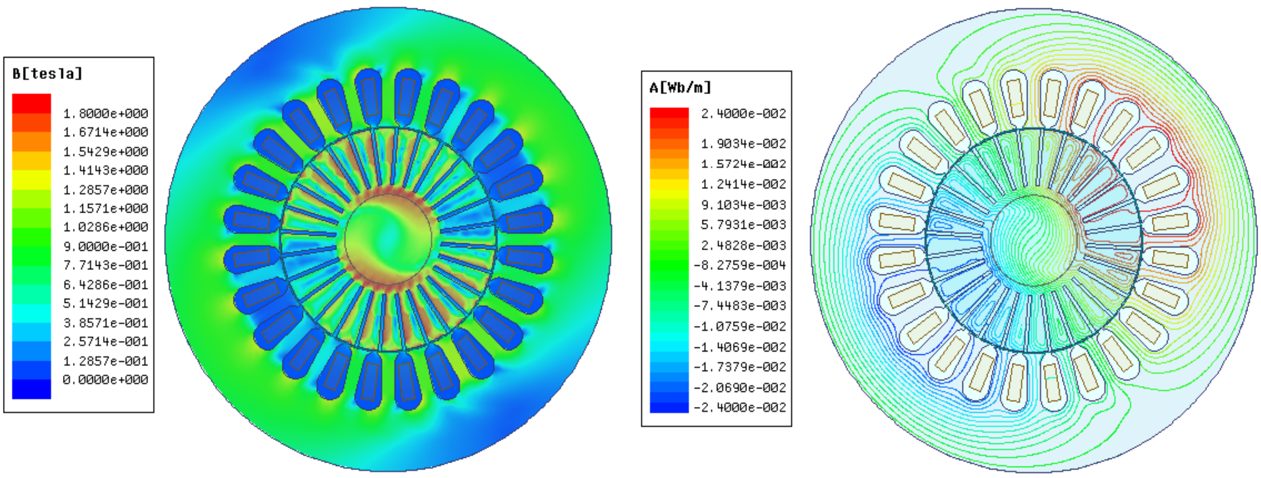

Fig. 9. Magnetic field density and magnetic flux lines distribution of ASSRIM with 0.25 mm slit width

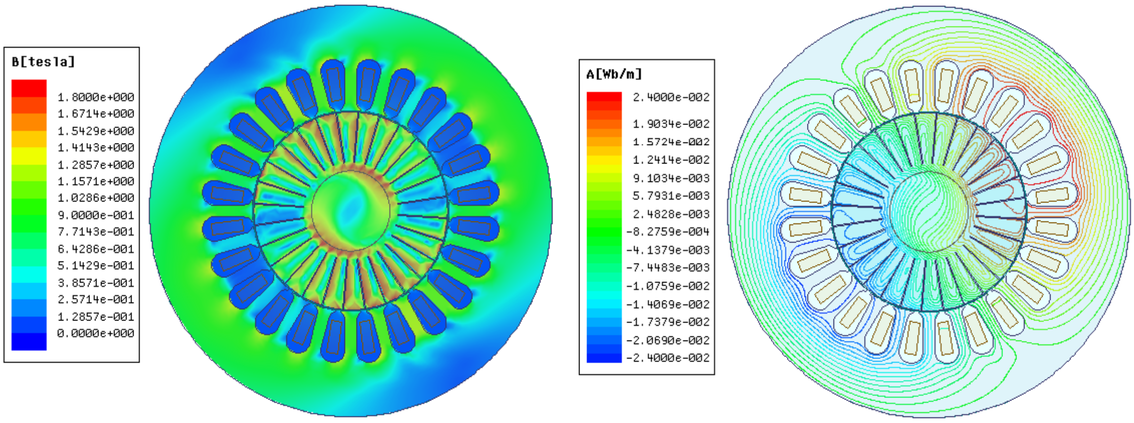

Fig. 10. Magnetic field density and magnetic flux lines distribution of ASSRIM with 1.5 mm slit width

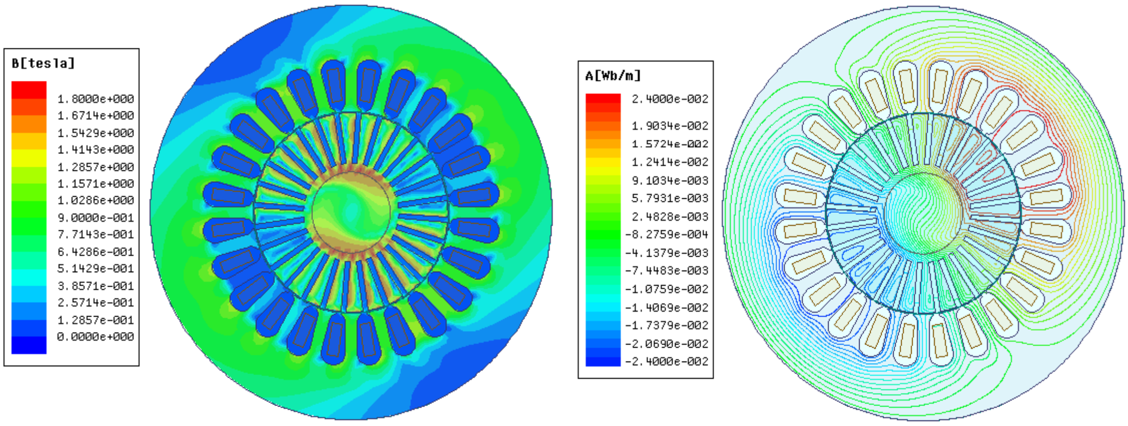

Fig. 11. Magnetic field density and magnetic flux lines distribution of ASSRIM with 2.5 mm slit width

5. Conclusion

In this study, 20.5 kW, 23600 min^{-1} high-speed ASSRIM have been designed based on previously designed 15.5 kW, 23600 min^{-1}, 225 V, 400 Hz high-speed SSRIM. Geometric parameters of slits such as slit depth and slit width have been optimized by FEM. In order to determine optimal geometrical parameters, firstly, slit depth is optimized and then slit width is optimized while keeping the optimized slit-depth constant.

Initial slitted design has 28 slits with 1.5 mm width. In order to optimize slit depth, 12 different slit depths have been analyzed at constant slit number and slit width by means of FEM. FEA results have shown that the optimal slit depth occurs at quarter of the diameter of the rotor since maximum electromagnetic torque with minimum supply current is seen at 25 mm slit depth. Afterwards, in order to find the optimum slit width for previously designed SSRIM, analyses have been made for 10 different slit widths with optimum slit depth 25 mm and 28 slits. Minimum input current with maximum electromagnetic torque has occurred at slit width of 1.5 mm for optimal design.

6. References

[1] G. Pasquarella, "Über die Entwicklung Einer Scnellaufenden Asynchronmaschine für Magnetgelagerte Hochgeschwindigkeits - Antriebe Erhöhter Leistung", Ph.D. thesis, ETH Zürich, Zürich, Switzerland, 1993.

[2] J. Huppunen, "High-Speed Solid-Rotor Induction Machine — Electromagnetic Calculation and Design", Ph.D. thesis, LUT, Lappeenranta, Finland, 2004.

[3] Y. G. Mekuria, "Development of a High Speed Solid Rotor Asynchronous Drive Ded by a Frequency Converter System", Ph.D thesis, TU Darmstadt, Darmstadt, Germany, 2013.

[4] R. Lateb, J. Enon, L. Durantay, "High Speed, High Power Induction Motor Technologies for Integrated for Compressors", *12th International Conference on Electrical Machines and Systems*, Tokyo, Japan, 2009, 5 pages, CD-ROM.

[5] H. A. Toliyat, G. B. Kliman, "Handbook of Electric Motors", Marcel Dekker Inc., Boca Raton, USA, 2004.

[6] P. K. Rajagopalan, M. V. Balarama, "Effects of Axial Slits on the Performance of Inductions Machines with Solid Rotors", *IEEE Trans. On Power Apparatus and Systems*, Vol. PAS 88, pp. 1695-1709, Nov., 1969.

[7] J. Saari, "Thermal Analysis of High-Speed Induction Machines", Ph.D thesis, TKK, Espoo, Finland, 1998.

[8] A. H. Oguz, "Kütle Rotorlu Asenkron Motor Tasarımı ve Veriminin İyileştirilmesine Yönelik Katkılar", Undergraduate thesis, ITU, Istanbul, Turkey, 2015.

[9] S. Nandi, S. Ahmed, H. A. Toliyat, "Detection of Rotor Slot and Other Eccentricity Related Harmonics in a Three

Phase Induction Motor with Different Rotor Cages", *IEEE Transaction on Energy Conversation*, vol.16, no.3, pp. 253-260, Sep., 2001.

[10] M. E. Zaim, "Non-Linear Models for the Design of Solid Rotor Induction Machines", *IEEE Transaction on Magnetics*, vol.35, no.3, pp. 1310-1313, May., 1999.

[11] R. L. Russell, K. H. Norsworthy, "Eddy current and wall losses in screened rotor induction motors", Proc. of IEE, vol. 105A, no. 20, pp. 163 173, Apr., 1958.